



Geochemistry

Textural and geochemical characteristics of the Ajali Sandstone, Anambra Basin, SE Nigeria: Implication for its provenance

*Caractéristiques texturales et géochimiques du grès d'Ajali, bassin d'Anambra, Sud-Est du Nigeria : implications de provenance*Moshood Niyi Tijani^{a,*}, Matthew Essien Nton^a, Ryuji Kitagawa^b^a Department of Geology, University of Ibadan, 200005 Ibadan, Nigeria^b Department of Earth and Planetary Sciences, Hiroshima University, 1-3-1 Kagamiyama, 739–8526, Hiroshima, Japan

ARTICLE INFO

Article history:

Received 27 November 2008

Accepted after revision 23 August 2009

Available online 6 February 2010

Presented by Zdenek Johan

Keywords:

Textural parameters

Geochemical characteristics

Weathering indices

Provenance

Ajali sandstone

Anambra basin

SE Nigeria

ABSTRACT

This study presents the mineralogical, textural and geochemical characteristics of the regional Maastrichtian Ajali Sandstone in Anambra Basin, SE Nigeria. The intent is to highlight possible constraints on the chemical weathering conditions of the source materials on one hand, and to infer the provenance on the other hand. The investigation approach involved field studies and collection of samples from 12 different outcrop locations, followed by laboratory studies involving grain-size analysis (GSA), major and trace elements analyses using the X-ray fluorescence (XRF) method as well as thin section petrography. Field studies show that the sandstones are friable at all locations and range in color from white in freshly cut stone, to reddish brown on weathering. In addition, the sandstone units are cross-bedded and show graded bedding exemplified by fining upward sequence. Textural examination indicates that the sandstones range from fine to medium sands, constituting about 76 to 99% sand fraction, with graphic mean grain size of 0.23 to 0.53 mm. Standard deviation (sorting) ranges from 0.56 to 1.24 ϕ and implies moderately well sorted sediments. Inferred from the textural indices, the depo-environmental discrimination of the Ajali Sandstone revealed a fluvial/river system-dominated sedimentary process. The sandstones are quartz arenite with quartz greater than 90% and less than 5% K-feldspar which indicate a predominant basement source as also revealed by the heavy mineral assemblages. In addition, major elemental oxides shows SiO₂ content greater than 96% for the fresh Ajali Sandstone samples with extreme depletion of mobile oxides such as Na₂O, CaO and the ferromagnesian minerals through weathering and sedimentary processes. Provenance and tectonic setting discrimination using geochemical data and compositional maturity revealed typical felsic igneous-dominated cratonic environment while inter-elemental ratios (such as Zr/Cr, Y/Ni, Th/Sc, La/Sc and La/Co) and ternary plots (e.g. Th–Sc–Zr; La–Th–Sc and Th–Co–Zr) reflect passive continental margin setting for the Ajali Sandstone. Consequently, the source area is constrained to the Precambrian basement rock units of Adamawa–Oban massif areas to the east of the Anambra Basin and the adjacent Abakaliki Anticlinorium.

© 2009 Académie des sciences. Published by Elsevier Masson SAS. All rights reserved.

* Corresponding author.

E-mail address: tmoshood@yahoo.com (M.N. Tijani).

R É S U M É

Mots clés :

Paramètres texturaux
 Caractéristiques géochimiques
 Index d'altération
 Provenance
 Grès d'Ajali
 Bassin d'Anambra
 SE Nigeria

Cette étude présente les caractéristiques minéralogiques, texturales et géochimiques du grès maastrichtien de la région d'Alali, bassin d'Anambra, Sud-Est Nigeria. Son but est de mettre en évidence les contraintes possibles, sur les conditions d'altération des matériaux source d'une part, et d'en inférer la provenance, d'autre part. La méthode d'approche comporte des études de terrain, la récolte d'échantillons à partir de 12 affleurements, suivies d'examen de laboratoire comportant analyse granulométrique, analyser des éléments majeurs et en traces utilisant la fluorescence X, analyse pétrographique sur lame mince. Les études de terrain montrent que le grès est friable sur tous les sites et que la couleur va du blanc sur la roche fraîche au brun rougeâtre sur les échantillons altérés. En outre, les formations présentes montrent stratification entrecroisée et granoclasement que la séquence fini-somitale illustre particulièrement bien. Du point de vue textural, les grès se révèlent constitués de sables fins à moyens représentant 76 à 99 %, avec une taille de grain moyenne de 0,23 à 0,53 mm. La déviation standard (classement) est comprise entre 0,56 et 1,24 ϕ et implique des sédiments modérément bien triés. Le grès d'Ajali révèle un mode de sédimentation dominé par un système fleuve/rivière. Les grès sont des arénites quartzieuses avec plus de 90 % de quartz et moins de 5 % de feldspath-K, ce qui indique une provenance prédominante du socle, comme l'indique l'assemblage de minéraux lourds. En outre, le contenu en oxydes d'éléments majeurs est de plus de 96 % de SiO_2 pour le grès frais et on observe un extrême appauvrissement en oxydes mobiles tels Na_2O et CaO et en ferromagnésiens au cours des processus d'altération et de sédimentation. La distinction entre provenance et mise en place tectonique d'après les données géochimiques et la maturité de composition révèle un environnement cratonique typique, dominé par les roches ignées, tandis que les rapports entre éléments tels que Zr/Cr , Y/Ni , Th/Sc , La/Sc et La/Co ou les points ternaires tels Th-Sc-Zr , La-Th-Sc et Th-Co-Zr reflètent la mise en place d'une marge continentale passive pour le grès d'Ajali. En conséquence, la région source est contrainte aux formations rocheuses du socle précambrien des zones du massif Adamawa-Oban à l'est du bassin d'Anambra et de l'anticlinorium d'Abakaliki.

© 2009 Académie des sciences. Publié par Elsevier Masson SAS. Tous droits réservés.

1. Introduction

Sandy sedimentary units are important parts of sedimentary basins throughout the world. Such units, either consolidated or unconsolidated, are known to be prolific sources of groundwater as well as important reservoir rocks in most petroleum provinces. It is widely known that, the textural characteristics of such sand units are products of weathering, transportation and sedimentary processes, while the compositions also depend on the primary chemical composition of the source rock area and the tectonic setting of the depositional basins (Bhatia and Crook, 1986; Das and Haake, 2003; Jin et al., 2006). Hence, composition of siliciclastic sedimentary rocks has been employed as sensitive indicator for provenance and weathering conditions at the source of sediments (Roser and Korsch, 1986, 1988; Goetze, 1998; Cullers, 2000; Getaneh, 2002; Ohta, 2004; Huntsman-Mapilaa et al., 2005). Furthermore, McLennan et al. (1983) and Taylor and McLennan (1985) noted that concentrations of major, trace and rare earth elements (REE) of sediments are well suited to constrain provenance and source rock composition due to the fact that the REE are transferred with minimal fractionation from the source material into sediments. Consequently, elemental ratios such as La/Sc , La/Co , Th/Sc and Zr/Cr have been found to be good discriminators between mafic and felsic source rocks as La , Th and Zr are said to be more concentrated in felsic igneous rocks while Co , Sc and Cr have higher concentrations in mafic rocks (Ronov et al., 1974; Wronkiewicz and Condie, 1987, 1990).

The Maastrichtian Ajali Sandstone, which is the focus of this study, is of particular importance due to its regional and aquiferous potential in terms of groundwater resources. Consequently, there are quite a number of existing studies focusing on aspects of groundwater resources of the Ajali Sandstone ranging from groundwater exploration to development and even hydrochemical quality aspects of the groundwater (Okagbue, 1988; Uma and Onuoha, 1988). In addition, several authors over the years have utilized sedimentological studies with the associated primary and biogenic structures to deduce the provenance and characterize the depositional environment of the Ajali Sandstone (Hoque and Ezepeue, 1977; Ladipo, 1986, 1988). However, no detail study of textural and geochemical constraints on provenance and tectonic setting has been carried out. Hence, this study focus on the use of textural, mineralogical and geochemical characteristics (including major and trace elements geochemistry) in the assessment of the provenance and tectonic setting of the source area of the Ajali Sandstone. Consequently, the objectives of this study are:

- to present new chemical and textural analytical data of the Maastrichtian siliciclastic sediments of Ajali Sandstone in Anambra Basin, SE Nigeria;
- to assess the possible weathering conditions at the source area;
- to infer possible provenance of the Ajali Sandstone based on the petrography, major and trace elements geochemistry as well as the weathering conditions at the source area.

2. Geologic and stratigraphic setting

The Ajali Sandstone is one of the lithostratigraphic units in the Anambra Basin, SE Nigeria. The Anambra Basin is an Upper Cretaceous (Maastrichtian) sedimentary basin located in the southeastern portion of Nigeria and bounded by the Lower Benue Trough to the east and by the Basement Complex of the southwestern Nigeria to the west. The origin of the Anambra Basin is closely related to the evolution of the Benue Trough, which in turn is associated with the separation of African from the South-American plate in the Mesozoic.

The general geological map of the Upper Cretaceous sedimentary succession within the Anambra Basin is presented in Fig. 1. The sedimentological and stratigraphic settings of the sediments within the Anambra Basin are defined by three main evolutionary stages.

2.1. First phase

The first phase defines a Pre-Santonian history, characterized by a strong subsidence in the Abakaliki domain of the Benue Trough, while the Anambra domain remained a platform where mud was deposited in a shallow restricted marine environment.

2.2. Second phase

The second phase, which commenced in the post-Santonian period, is characterized by the uplift of the Abakaliki sub-basin of the Benue Trough, and the subsidence of the Anambra platform characterized by a shallow marine system. This resulted in the deposition of the Nkporo/Enugu shales and Lower Coal Measures (Mamu Formation), followed by a regressive fluvio-deltaic system during the Maastrichtian, leading to the deposition of the regional Ajali Sandstone and Nsukka Formation.

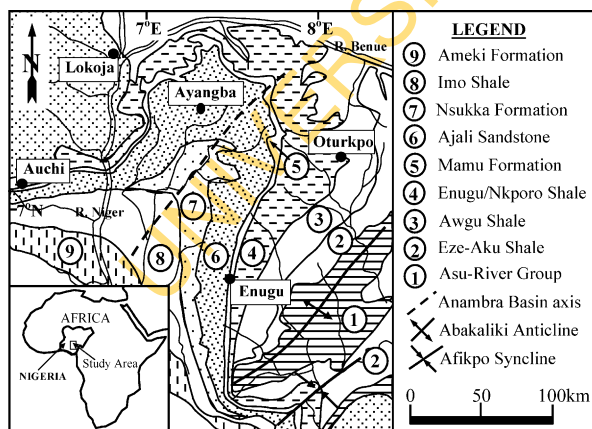


Fig. 1. Geological Map of Anambra Basin showing the different sedimentary units (Inset: showing location of Nigeria and the Anambra Basin).

Fig. 1. Carte géologique du bassin d'Anambra montrant les différentes unités sédimentaires (encart montrant la localisation du Nigeria et du bassin d'Anambra).

2.3. Last phase

The last phase occurred during the Lower Tertiary and was marked by the development of the Niger Delta, which prograded along the Anambra Basin axis. This was characterized by the deposition of Imo shale and Bende-Ameki Groups, especially in the southern part of the Anambra sub-Basin during the Paleocene and Eocene periods respectively.

A detailed stratigraphic relationship of the sedimentary units as outlined above is presented in Fig. 2, while further details of the stratigraphic setting, sedimentation history and tectonic evolution of the Anambra Basin can be found in the works of Reyment, 1965; Murat, 1972; Hoque and Ezepeue, 1977; Benkheilil, 1986 and Ladipo, 1988.

Previous studies of the Ajali Sandstone, which forms the focus of this study, have suggested continental and fluvio-deltaic setting as a regressive phase of a short-lived Maastrichtian transgression. The sediments were derived from westerly areas of the Abakaliki anticlinorium and the granitic basement units of Oban and Adamawa massifs (Benkheilil, 1986; Amajor, 1987, Adediran et al., 1991). However, based on the presence of trace fossils (*Ophiomorpha* and *Skolithos*) and other sedimentary structures, Ladipo (1986) suggested a tidal shallow marine depositional environment for the Mamu Formation and the overlying Ajali Sandstone, as part of a continued Maastrichtian transgression, which commenced in the Late Campanian and lasted until the Paleocene. However, outcrops of Ajali Sandstone extend from Fugar/Agenebode area in the west, towards Enugu/Udi area in the east and narrows southwards towards Okigwe area, thereby forming a characteristic “question mark” shape (Fig. 3). The thickness ranges from over 350 to 450 m in places and thins southward to few tens of meters around Okigwe area (Hoque and Ezepeue, 1977).

Field study shows that the Ajali Sandstone consists of friable medium- to fine-grained sands, averagely sorted, typically whitish in colour (occasionally iron-stained in places) with characteristic cross-stratification, thus the common reference as false-bedded sandstone (Tattam, 1944; Simpson, 1955). Plate 1a shows a representative expression of the whitish Ajali Sandstone outcrop with cross-stratification features as observed in road cuts/quarry pits within the study area. Also field observation revealed that the upper portion of the Ajali Sandstone is ferruginized in places with weathering front defined by the extent of infiltration/recharge water as shown in Plate 1b. Furthermore, recent laboratory study (Tijani and Nton, 2009) revealed porosity of 18.3 to 32.8% (av. 27%) and average K-value of 1.4×10^{-3} m/sec, which falls within the range of 10^{-5} and 10^{-3} m/sec for fine to medium sands. This is an indication of good aquiferous potentials of the Ajali Sandstone and higher recharge/infiltration rate within the outcrop areas.

3. Methodology

A geological field survey of the study area involved collection of representative samples from 12 different

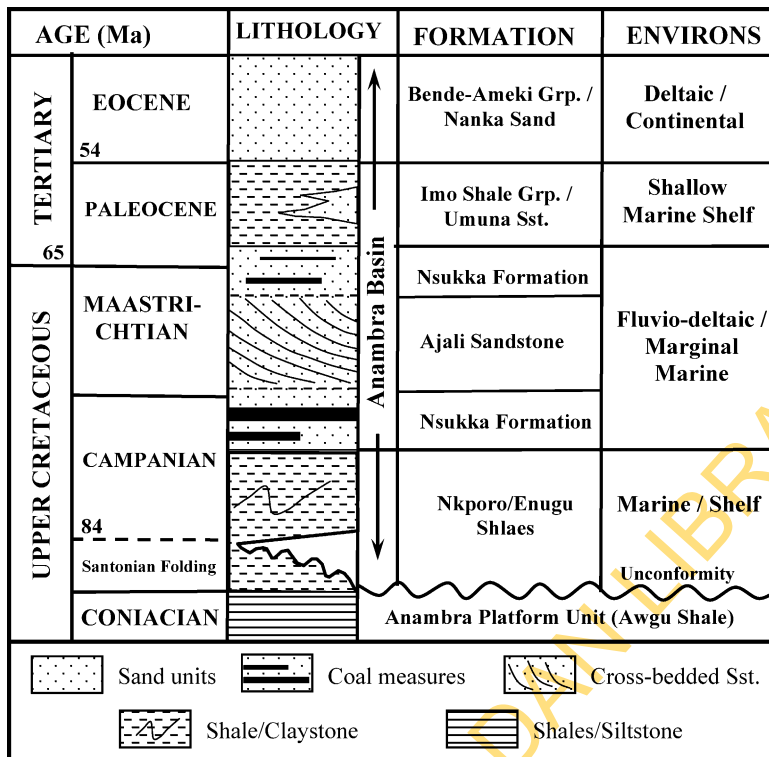


Fig. 2. Stratigraphic profiles and depositional environment of the sedimentary units within the Anambra Basin Nigeria.

Fig. 2. Profils stratigraphiques et environnement de dépôt des unités sédimentaires à l'intérieur du bassin d'Anambra.

locations within the outcropping areas of the Ajali Sandstone in the Anambra Basin as shown in Fig. 3. This was complemented by detail examination of the lithostratigraphic profiles of the exposure at the different sampling locations.

However, it should be noted that the limitation of the sampling locations to 12 representative outcrop areas was consequent to the relatively uniform or homogenous characteristics of the Ajali Sandstone at all the different outcrop locations. Subsequent to the field sampling operations, the first phase of the laboratory studies involved grain-size analysis (GSA) and thin-section petrography/heavy mineral studies conducted at the Sedimentological Laboratory of the Department of Geology, University of Ibadan, Nigeria. The second phase involved major and trace elements geochemical analyses, which were carried out at the Department of Earth and Planetary Science Systems, Hiroshima University, Japan.

For the GSA, the samples were sun-dried and then disaggregated with hands due to loose friable nature of the Ajali Sandstone. The samples were subsequently weighed and sieved for particle-size distribution following standard laboratory procedures using a Ro-tap shaker machine. From the GSA results, respective cumulative curves were plotted followed by determination of statistical parameters such as sorting, skewness, and kurtosis based on the concept of Folk and Ward (1957) and Folk (1974). For the mineralogical study, six representative fresh samples of the Ajali Sandstone were selected for thin-section petrography. The samples were impregnated with resin

before cutting and mounting on slides with araldite and Canada balsam. The point-counting method, according to Ingersoll et al., 1984 and Osaie et al., 2006 was employed for quantitative compositional analysis of the different mineral grains. This has the advantage of minimizing compositional dependence on grain sizes as sandstones of different sizes can be compared. The modal analysis was also performed by counting more than 300 points per thin section as reported by Gazzi (1966) and Dickinson (1970), while the slides were examined under the flat stage of a petrological microscope and classified based on Folk (1974). Similarly, bromoform extracts of accessory minerals were mounted on slides and examined for their non-opaque fractions.

The determination of the major and trace elements composition of the Ajali Sandstone was carried out using X-ray fluorescence (XRF) methods. Sixteen fresh and four weathered samples were subjected to appropriate treatment by homogenization of 2 g of each sample with 4 g of analytical *spectroflux* powder and 0.6 g LiNO₃ salt in agate mortar. The respective mixture was subjected to heat-fusion and glass beads preparation in platinum plate (3.5 cm diameter) using bead and fuse sampling machine (model TK-410, Rigaku-Tokyo). Subsequently, the respective glass beads were used for the determination of major and trace elements using automated XRF machine (model Rigaku ZSX). Finally, data evaluations employed in this study include estimations of elemental ratio and cross-plots (for the assessment of compositional characteristics), evaluation of mineralogical maturity and weathering

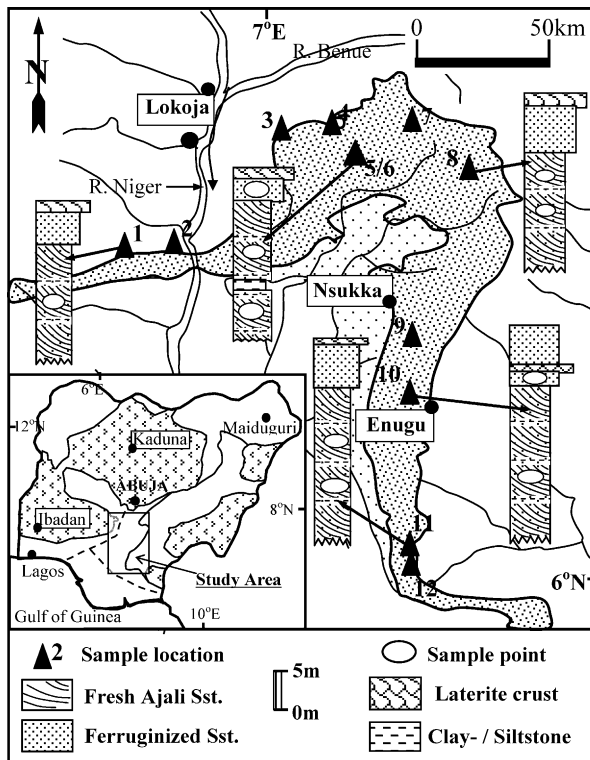


Fig. 3. Geological Outcrop Map of the Ajali Sandstone showing the different sample locations and representative lithologies (Inset: Map of Nigeria showing the location of Anambra Basin).

Fig. 3. Carte des affleurements géologiques du grès d'Ajali montrant la localisation des échantillons étudiés et les logs représentatifs (encart : carte du Nigeria montrant la localisation du bassin d'Anambra).

indices (for the assessment of source area weathering conditions), ternary and discriminant plots (for assessment of provenance and tectonic settings).

4. Results and interpretations

4.1. Granulometric and textural studies

The plots of representative samples of the grain-size distribution curves of the Ajali Sandstone samples from different outcrop locations within the Anambra Basin are presented in Fig. 4, while the results of the estimated textural and statistical indices are presented in Table 1. As shown in Table 1 and also graphically presented in Fig. 4, the Ajali Sandstone falls predominantly within uniform medium-sand range. This is clearly supported by the graphic mean (G_m) of 0.98–1.98 phi; with the exception of sample from Dekina, having graphic mean of 2.26 phi, which implies fine sand. Estimated inclusive graphic standard deviation (D) ranges from 0.55 to 1.29 phi suggesting a wider range from poorly sorted to moderately well-sorted material. Also, varied values of inclusive graphic skewness from -0.24 to $+0.20$ (av. 0.02) imply nearly symmetrical to coarse skewed arrangement while graphic kurtosis (KG) ranges from 0.94 to 1.51 phi (av.

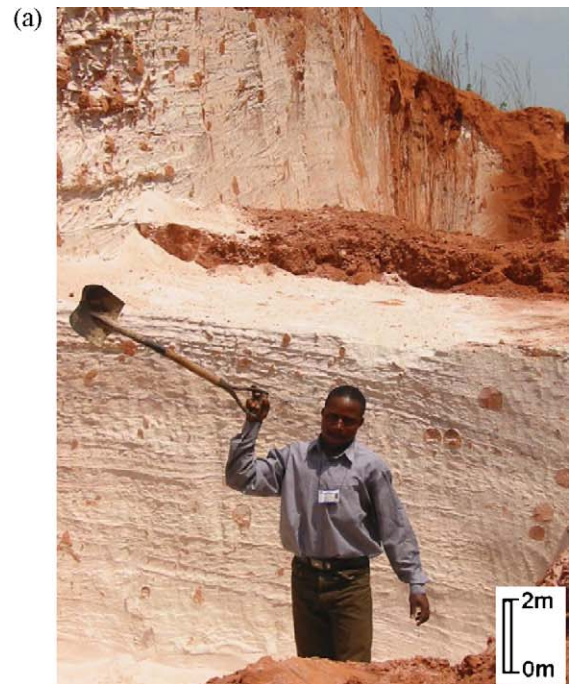


Plate 1. a : photo-image of representative outcrop of the whitish Ajali Sandstone showing cross-stratification features as observed in quarry pits; b : photo-image of ferruginized upper portion of the Ajali Sandstone showing the extent of weathering front as defined by percolating/recharge water.

Plate 1. a : photo d'un affleurement représentatif de grès d'Ajali montrant des traits de stratification entrecroisée, tels qu'on les observe en carrière ; b : photo de la portion supérieure ferruginisée du grès d'Ajali montrant le développement du front d'altération par action de l'eau de recharge/percolation.

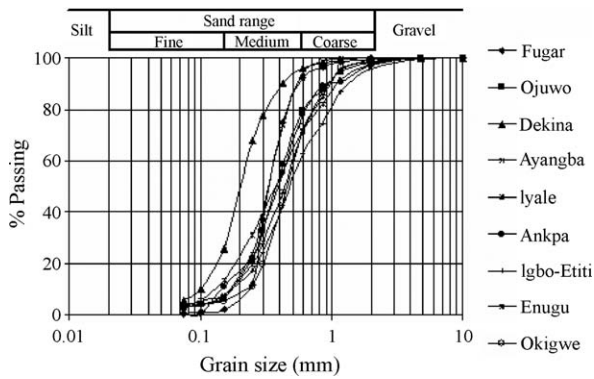


Fig. 4. Representative grain-size distribution curves of the Ajali Sandstone.

Fig. 4. Courbes représentatives de répartition des tailles granulométriques du grès d'Ajali.

1.20) and suggests mesokurtic through leptokurtic with majority of the samples having leptokurtic population.

Generally, with the exception of sample from Okigwe-Uturu 1, percentage fines for all other samples ranges from 0.30 to 6.0, with percentage sand of greater than 94% (Table 1). Statistical parameters from textural studies of granular sediments have been successfully employed in sedimentology to reveal the transportation history, sedimentary processes as well as the characteristics of the depositional environments (Folk and Ward, 1957; Folk, 1974; Friedman, 1967, 1969; Olugbemiro and Nwajide, 1997). In this study, from the plots of simple skewness against standard deviation (sorting) (Fig. 5A), as well as that of mean grain size against standard deviation (Fig. 5B), it is clearly shown that the Ajali Sandstone samples are of river sand and fluvial in origin. This is based on the concept of Friedman (1969) and Folk (1974) respectively.

4.2. Petrographic study

Initial mineralogical examination under binocular microscope of selected fresh Ajali Sandstone sample

Table 1

Results and summary of statistical and textural indices based on GSA data for the fresh Ajali Sandstone samples.

Tableau 1

Résultats et résumé des indices texturaux et statistiques basés sur des données GSA pour les échantillons de grès d'Ajali frais.

Sample code	Location	Gmean (phi)	IGStd. (phi)	IGSkw.	Gkurt.	% Fine	% Sand
AJSt-01	Fugar-Agenebo-I	1.48	0.55	0.20	1.51	0.6	99.4
AJSt-02	Fugar-Agenebo-II	1.96	0.61	0.18	0.94	1.6	98.4
AJSt-03	Ojuwo	1.41	0.94	0.01	1.22	3.0	97.0
AJSt-04a	Dekina-I	2.26	0.82	0.07	1.40	6.0	94.0
AJSt-05a	Ayangba-Ia	1.63	0.70	-0.24	1.38	3.1	96.9
AJSt-05b	Ayangba-Ib	1.43	0.74	0.12	1.02	1.4	98.6
AJSt-07	Iyale	1.36	1.28	0.04	0.99	3.8	96.2
AJSt-08	Ankpa	1.45	1.07	-0.01	1.38	0.3	99.7
AJSt-09a	Igbo-Etiti-I	1.29	1.29	-0.05	1.23	4.3	95.7
AJSt-10a	Enugu-Km8-Ia	1.21	1.01	-0.10	0.96	2.8	97.2
AJSt-12	Okigwe-Uturu-I	1.69	0.64	ND	ND	24.9	75.1
AJSt-13a	Okigwe-Uturu-IIa	1.10	0.87	-0.04	1.34	3.4	96.6
	Minimum	0.98	0.55	-0.24	0.94	0.3	75.1
	Maximum	2.26	1.29	0.20	1.51	24.9	99.7
	Mean	1.50	0.88	0.02	1.20	4.6	95.4

Gmean: graphic mean (phi); IGStd: inclusive standard deviation (phi); IGSkew: inclusive graphic skewness; Gkurt: graphic kurtosis.

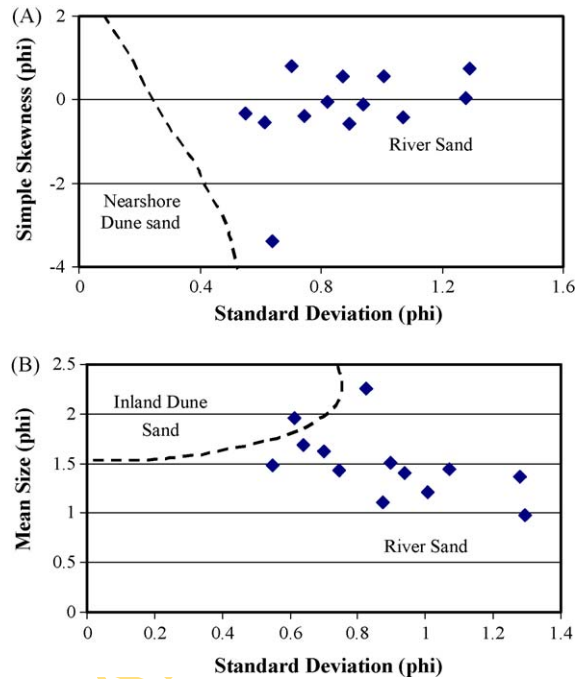


Fig. 5. Depo-environmental discrimination of Ajali Sandstone. A. Simple skewness against Standard Deviation. B. Mean Grain Size against Standard Deviation.

Fig. 5. Discrimination dépo-environnementale du grès d'Ajali. A. Simple obliquité en fonction de la déviation standard. B. Granulométrie moyenne en fonction de la déviation standard.

revealed the dominance of sub-angular to rounded polycrystalline quartz in the samples while the presence of dispersed whitish fines suggests limited clay cementing material. Based on the petrologic assessment, the Ajali Sandstone samples revealed mainly moderately well sorted materials while the framework grains are composed of monocrystalline quartz, polycrystalline quartz, K-feldspar and rock fragments (Table 2). A further highlight of the petrographic feature of the Ajali Sandstone is

Table 2

Petrographic analysis data for fresh Ajali Sandstone samples.

Tableau 2

Données de l'analyse pétrographique pour les échantillons de grès d'Ajali frais.

Sample No.	Location	CQ	MQ	Fsp	Rf.	Matrix	Cement	% Qt	% Fsp	% Rf	MMI
AJ St-01	Fugar-Agenebode-1	79	12.0	4.7	1.4	2.0	0.9	93.7	4.8	1.4	0.94
AJ St-04a	Dekina-1	83	7.0	3.5	2.5	2.9	1.1	93.8	3.6	2.6	0.94
AJ St-05a	Ayangba-1a	77	15.0	3.5	2.0	2.0	0.5	94.4	3.6	2.1	0.94
AJ St-09a	Igbo-Etiti-1	84	5.7	5.0	3.1	2.2	0.7	91.7	5.1	3.2	0.91
AJ St-10a	Enugu-Km8-1a	83	10.0	2.9	0.8	2.7	0.6	96.2	3.2	0.8	0.96
AJ St-12	Okigwe-Uturu-1	86	7.0	3.3	2.1	0.8	0.8	94.5	3.4	2.1	0.94
	Average	82	9.5	3.8	2.0	2.1	0.8	94.1	4.0	2.0	0.94

CQ: common quartz; MQ: metamorphic quartz; Fsp.: feldspar; Rf.: rock fragment; Qt: total quartz; MMI: mineralogical maturity index ($Qt / [Qt + Fsp + Rf]$) after Bhatia and Crook, 1986.

presented in [Plate 2a](#) showing (in cross nicol) quartz-dominated sub-rounded to rounded grains (Q) in quartz arenite of fresh Ajali Sandstone sample. However, [Plate 2b](#) presents photographic image of ferruginized Ajali Sandstone showing poorly sorted sub-rounded quartz grains and ferruginized matrix.

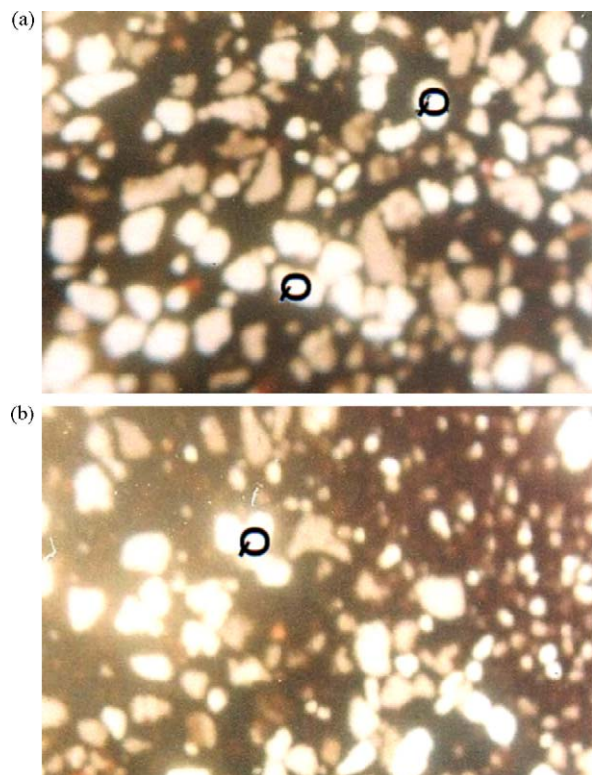


Plate 2. a: photomicrograph showing (in cross nicol) quartz-dominated sub-rounded to rounded grains (Q) in quartz arenite of fresh Ajali Sandstone sample (X 40); b: photographic image showing (in cross nicol) sub-rounded to rounded grains in quartz arenite of ferruginized Ajali Sandstone. (Note: poor sorting and ferruginized matrix; X 40).

Plate 2. a : microphotographie entre nicols croisés montrant la prédominance de grains de quartz(Q) sub-ronds à ronds dans l'arénite quartzreuse du grès frais d'Ajali (X 40) ; b : microphotographie entre nicols croisés montrant la prédominance de grains de quartz sub-ronds à ronds dans l'arénite quartzreuse du grès ferruginisé d'Ajali (à noter le mauvais classement de la matrice ferrugineuse) : (X 40).

On the basis of the observed mineralogical composition and the estimated mineralogical maturity index (MMI) of 0.91 to 0.94, the Ajali Sandstone is classified as quartz arenite. Quartz, as the most abundant framework grain in the Ajali Sandstone, constitutes on the average 90% by rock volume. The grains are sub-angular to sub-rounded in shape; however, the monocrystalline quartz dominates over the polycrystalline type. The monocrystalline quartz shows straight to slightly undulose extinction while the polycrystalline quartz shows strong undulose extinction.

The feldspars are mainly dominated by K-feldspar over plagioclase while the rock (lithic) fragments are comparatively less abundant and are dominantly of sedimentary and metamorphic origin. The slight dominance of K-feldspar over plagioclase and very low lithic fragments are indications of either prolonged weathering, transportation or recycling as also noted by Akarish and El-Gohary (2008). Heavy minerals show rounded zircon and other minerals such as tourmaline, garnet and rutile, all of which commonly occur as silt-size fraction. The overall petrologic assessment revealed that the observed quartz arenites can be described as mature sandstone that was derived from primary basement rocks with some intrabasinal recycling (apparently from the adjacent Abakaliki Anticlinorium) as suggested by the presence of some sub-rounded to rounded heavy mineral grains.

4.3. Major element distribution

The results of the major elemental distribution for both fresh and ferruginized Ajali Sandstone samples are presented in [Table 3](#), alongside with the estimated weathering indices. As shown in [Table 3](#), the analyzed samples are dominated by silica with 94.8 to 99.0 wt.% SiO_2 , while other major oxides are generally below 1.0 wt.% in the fresh samples. The results generally revealed similar elemental composition for all samples reflecting the homogeneity of the Ajali Sandstone. This may be attributable to uniform depositional conditions for the sediments. However, the ferruginized samples, though with similar chemical trends exhibit elevated concentrations of Al_2O_3 (3.50–11.60 wt.%) and Fe_2O_3 (1.80–3.60 wt.%), which are clear indications of weathering processes. This is clearly supported by the low Si/Al ratio of 6.6 to 24.1 compared to the relatively higher values of 43.5 to 300 for the fresh samples.

Table 3
Results of the major elements analyses alongside with weathering indices.

Tableau 3
Résultats d'analyse des éléments majeurs, avec les indices d'altération.

Sample No.	Location	SiO ₂	Al ₂ O ₃	Fe ₂ O ₃	TiO ₂	MnO	MgO	CaO	Na ₂ O	K ₂ O	P ₂ O ₅	LOI	%CIA	%CIW
AJSt-01	Fugar-Agene-I	99.0	0.33	0.07	0.04	0.002	0.01	0.01	0.01	0.03	0.002	0.5	86.8	94.3
AJSt-02	Fugar-Agene-II	98.9	0.86	0.05	0.05	0.01	0.01	0.01	0.01	0.06	0.01	0.1	91.5	97.7
AJSt-04a	Dekina-I	97.1	1.12	0.29	0.26	0.01	0.01	0.01	0.01	0.01	0.01	1.2	97.4	98.2
AJSt-04b	Dekina-II	97.3	1.02	0.25	0.26	0.01	0.02	0.03	0.04	0.04	0.02	1.0	90.3	93.6
AJSt-05a	Ayangba-Ia	96.7	1.09	0.21	0.31	0.003	0.01	0.01	0.01	0.003	0.01	1.7	97.9	98.2
AJSt-05b	Ayangba-Ib	95.4	2.56	0.51	0.84	0.01	0.05	0.06	0.01	0.05	0.02	0.5	95.5	97.3
AJSt-06a	Ayangba-IIa	98.1	0.35	0.17	0.28	0.003	0.01	0.01	0.01	0.002	0.01	1.0	94.1	94.6
AJSt-06b	Ayangba-IIb	97.5	0.86	0.34	0.74	0.01	0.04	0.05	0.01	0.04	0.01	0.4	89.6	93.5
AJSt-08	Ankpa	98.9	0.71	0.04	0.05	0.01	0.01	0.01	0.03	0.04	0.01	0.2	89.9	94.7
AJSt-09a	Igbo-Etiti-I	94.8	2.18	0.59	0.26	0.002	0.01	0.01	0.01	0.01	0.01	2.1	98.6	99.1
AJSt-09b	Igbo-Etiti-II	96.4	1.71	0.46	0.06	0.01	0.01	0.03	0.04	0.04	0.01	1.3	94.0	96.1
AJSt-10a	Enugu-Km8-Ia	96.2	1.33	0.03	0.07	0.001	0.01	0.01	0.01	0.002	0.003	2.3	98.4	98.5
AJSt-10b	Enugu-Km8-Ib	96.7	1.7	0.29	0.12	0.01	0.01	0.02	0.03	0.08	0.01	1.1	92.9	97.1
AJSt-12	Okigwe-Uturu-I	97.3	0.92	0.17	0.19	0.002	0.01	0.01	0.01	0.004	0.01	1.4	97.5	97.9
AJSt-13a	Okigwe-Uturu-IIa	97.6	0.87	0.11	0.12	0.01	0.01	0.01	0.02	0.04	0.01	1.2	92.6	96.7
AJSt-13b	Okigwe-Uturu-IIb	97.8	0.87	0.1	0.12	0.01	0.01	0.02	0.01	0.04	0.01	1.0	92.6	96.7
AJSt-05c	Ayangba-III (W)	78.8	10.5	3.25	1.03	0.01	0.04	0.01	0.01	0.03	0.06	6.2	99.5	99.8
AJSt-11a	Enugu-Km8 (W)	91.4	3.79	1.94	0.42	0.01	0.02	0.01	0.01	0.01	0.02	2.4	99.2	99.5
AJSt-11b	Enugu-Km8 (W)	91.9	3.56	1.8	0.32	0.01	0.02	0.01	0.02	0.03	0.01	2.4	98.3	99.2
AJSt-14a	U-Okigwe IIIa (W)	76.8	11.57	3.57	1.03	0.01	0.04	0.01	0.01	0.03	0.06	6.9	99.6	99.8
AJSt-14b	U-Okigwe IIIb (W)	80.2	10.17	2.96	0.9	0.01	0.03	0.02	0.01	0.03	0.06	5.6	99.4	99.7
Modern Big Rivers (Potter, 1978)		85.3	7.45	2.76	0.78	0.05	1.02	1.12	0.23	1.14	0.02			
Arkose (Pettijohn, 1963)		80.2	9.04	2.37	0.31	0.28	0.52	2.81	1.56	2.91	0.10			
Buem Sst. Ghana (Osae et al., 2006)		94.52	0.20	3.34	0.01	0.02	0.08	0.11	0.05	–	0.01	0.44	97.0	

Ferruginized samples marked with (W). Ref. Sample: reference sample.

Arising from the ternary plots of the chemical composition using Silica–Sesquioxides–Alkalis as presented in Fig. 6A, it can be observed that all the samples lie towards the silica (SiO₂) corner thus indicating severe

depletion of the sesquioxides and the alkalis. This deduction is consistent with the Al₂O₃–CaO+Na₂O–K₂O ternary diagram (Fig. 6B), which shows the distribution of the Ajali Sandstone samples alongside with the primary mineralogy of typical Basement Complex rocks as reported in Tijani et al., 2006. As indicated, the Ajali Sandstone samples plot at the Al₂O₃ corner, thus implying intense primary weathering processes and removal of feldspars and other labile components that characterized the primary source rock materials.

Furthermore, the negative correlation of silica as shown in the cross plots of the % SiO₂ versus Fe₂O₃ (Fig. 7A); versus Al₂O₃ (Fig. 7B) and versus LOI (Fig. 7C) demonstrate influence of weathering processes through enrichment of silica and depletion of Fe and Mg as well as the decrease in LOI with increasing weathering and maturity of the sediments. The implication of marked negative correlation between SiO₂ and Al₂O₃ is also an indication of the fact that most of the silica is present as quartz grains. However, the positive correlation between Fe₂O₃ and Al₂O₃ (Fig. 7D) is an indication of a common source and suggests possible controls by the proportion of clay (fines) contents as products of weathering/ferruginization processes. It can be concluded, therefore, that the depletion of all other major elements in the Ajali Sandstone is related to the removal of ferromagnesian minerals and feldspars through reworking and transportation of the source materials by sedimentary processes.

4.4. Trace element distribution

The results of trace element concentrations of the analyzed Ajali Sandstone samples are presented in Table 4.

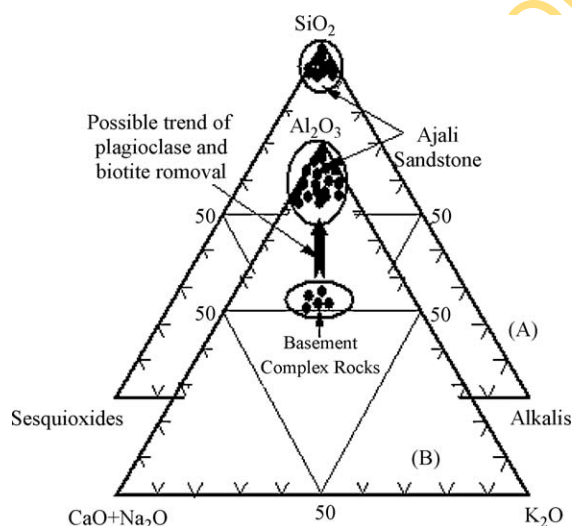


Fig. 6. Mineralogical and chemical composition of the Ajali Sandstone samples plotted on: A. Quartz–Sesquioxides–Alkalis. B. Al₂O₃–CaO + Na₂O–K₂O ternary diagrams. (Note: bold arrow indicates trend of plagioclase and biotite removal during weathering and transportation processes).

Fig. 6. Compositions minéralogique et chimique des échantillons de grès d'Ajali reportées en : A. Diagramme ternaire quartz-sesquioxides-alkalis. B. Diagramme ternaire Al₂O₃–CaO + Na₂O–K₂O (à noter que la flèche en gras indique la tendance à l'élimination du plagioclase et de la biotite au cours de l'altération et du transport).

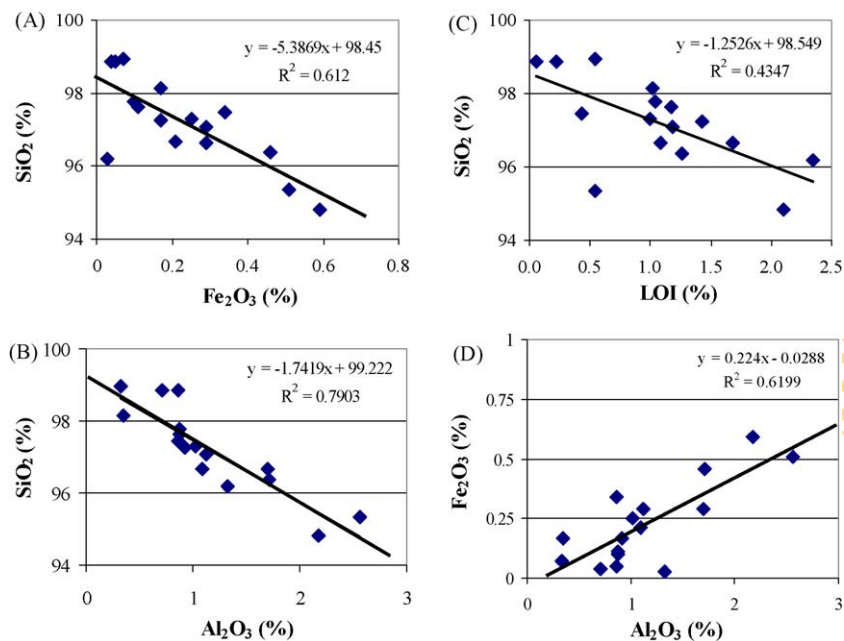


Fig. 7. Cross plots of major oxides: A. SiO₂ against Fe₂O₃. B. SiO₂ against Al₂O₃. C. SiO₂ against LOI. D. Fe₂O₃ against Al₂O₃.

Fig. 7. Diagrammes représentant les oxydes principaux. A. SiO₂ en fonction de Fe₂O₃. B. SiO₂ en fonction de Al₂O₃. C. SiO₂ en fonction de LOI. D. Fe₂O₃ en fonction de Al₂O₃.

Table 4

Trace metal concentrations in the analyzed Ajali Sandstone samples.

Tableau 4

Teneurs des métaux en trace dans les échantillons de grès d'Ajali analysés.

Sample No.	Location	Sc	V	Cr	Co	Ni	Cu	Zn	Ga	Rb	Sr	Y
AJSt-01	Fugar-Agene-I	0.1	3.75	5.46	0.01	2.3	0.01	4.36	0.93	1.15	8.17	0.87
AJSt-04a	Dekina-I	1.25	14.19	11.14	0.62	3.66	0.01	4.1	1.22	62.06	8.62	7.51
AJSt-05a	Ayangba-Ia	1.8	13.79	11.85	0.66	1.52	0.68	3.87	2.23	1.56	8.96	1.47
AJSt-06a	Ayangba-IIa	0.13	10.69	11.96	0.01	2.33	0.01	6.78	0.5	1.44	10.7	0.46
AJSt-09a	Igbo-Etiti-I	0.81	15.39	12.83	0.17	3.15	0.01	3.08	2.99	123.19	13.26	15.97
AJSt-10a	Enugu-Km8-Ia	0.13	4.4	5.09	0.01	2.13	0.01	2.66	0.71	51.52	7.14	7.4
AJSt-12	Okigwe-Uturu-I	0.84	12.3	7.64	0.08	2.6	2.16	5.72	1.37	0.67	11.01	0.6
AJSt-05c	Ayangba-III (W)	8.18	98.24	52.38	1.97	10.23	3.64	12.49	18.25	4.08	71.36	20.23
AJSt-11a	Enugu-Km8-Iia (W)	2.14	26.94	17.89	0.78	5.41	3.07	7.2	3.15	3.37	17.15	5.85
AJSt-14a	Okigwe-Uturu-IIIa (W)	8.18	107.04	58.48	2.79	12.36	3.73	15.18	15.73	3.56	75.01	17.44
	Mean (overall)	2.4	30.7	19.5	0.71	4.6	1.33	6.5	4.7	25.3	23.1	7.9
	Mean (fresh)	0.7	10.6	9.4	0.23	2.5	0.43	4.4	1.4	34.5	9.7	4.9

Trace metal concentrations (PPM) in the analyzed ASF samples											
Sample No.	Location	Zr	Nb	Ba	La	Ce	Nd	Yb	Hf	Pb	Th
AJSt-01	Fugar-Agene-I	45.9	4.29	23.58	3.98	7.48	3.28	0.01	0.62	2.05	2.62
AJSt-04a	Dekina-I	285.0	8.49	23.08	6.22	24.15	8.31	1.22	4.37	3.11	5.36
AJSt-05a	Ayangba-Ia	403.4	8.30	25.05	11.23	40.80	12.92	0.01	6.26	4.43	7.02
AJSt-06a	Ayangba-IIa	283.5	9.05	18.16	8.31	29.02	13.63	0.01	3.71	3.43	3.90
AJSt-09a	Igbo-Etiti-I	268.7	9.60	7.32	9.20	26.80	10.66	0.31	4.62	3.51	5.39
AJSt-10a	Enugu-Km8-Ia	121.2	5.47	16.43	3.94	14.38	5.29	0.01	1.52	2.14	6.88
AJSt-12	Okigwe-Uturu-I	172.8	7.55	24.83	5.12	20.75	7.25	0.01	2.98	2.68	5.45
AJSt-05c	Ayangba-III (W)	814.1	27.03	57.01	35.16	78.63	26.57	2.01	11.01	13.29	12.51
AJSt-11a	Enugu-Km8-Iia (W)	451.3	10.64	25.85	17.63	51.91	18.15	0.01	6.86	8.01	9.34
AJSt-14a	Okigwe-Uturu-IIIa (W)	795.3	28.01	58.06	32.14	85.86	29.97	2.05	13.10	15.62	14.85
	Mean (overall)	364.1	11.80	27.90	13.30	37.90	13.60	0.57	5.51	5.80	7.30
	Mean (fresh)	225.8	7.50	19.80	6.90	23.30	8.80	0.23	3.44	3.10	5.20

Due to their preferential enrichments in different rock types, relationships between the trace elements are usually exploited for discriminating the possible source rock (Wronkiewicz and Condie, 1987, 1990). As shown in

Table 4, the trace elements reveal relatively varied concentrations between fresh and ferruginized samples. Data for the fresh (unweathered) samples, revealed relative enrichment of some indicator elements such as

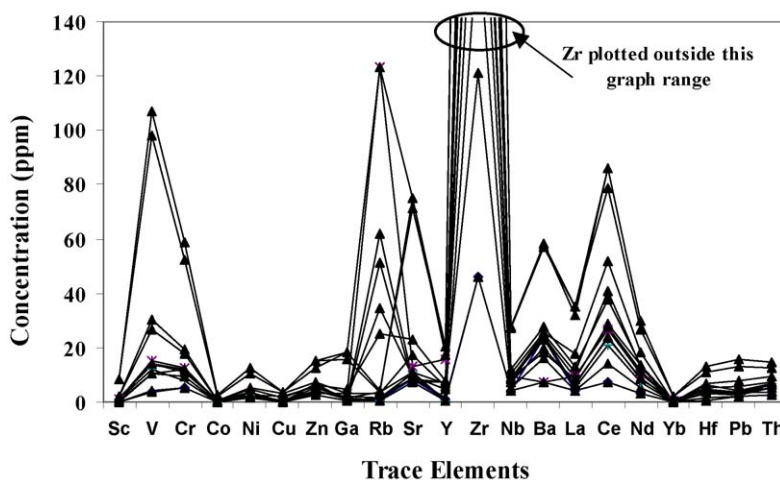


Fig. 8. Graphical plot of the Trace elements concentration in the Ajali Sandstone.

Fig. 8. Diagramme de concentration des éléments en traces dans le grès d'Ajali.

Zr, Cr, V, La, Th, Ba and Sr with average concentrations of 225.8 ppm Zr; 9.4 ppm Cr; 10.6 ppm V; 6.9 ppm La; 5.2 ppm Th; 19.8 ppm Ba and 9.7 ppm Sr (Table 4).

Such indicator elements and their relative enrichments in the Ajali Sandstone can also be attributed to the depletion of plagioclase and unstable fragments, leading to abundance of immobile elements during sedimentary processes. In addition, the abundance of high field strength elements (e.g. Cr, Zr, etc) can be related to the presence of detrital minerals such as chrome spinel, zircon, etc (Huntsman-Mapilaa et al., 2005). Although the plot of the trace elements profile as presented in Fig. 8 indicates variation within the samples, it clearly indicates similar trends for all the samples with enrichment of some indicator elements like V, Rb, Sr, Ba, Zr and Ce. Such enrichment is a strong indication of the relatively matured nature of the Ajali Sandstone as quartz arenite.

For the weathered or ferruginous samples, almost all the trace metals (with the exception of Rb) exhibit higher concentrations than those of the fresh samples (Table 4). Furthermore, the relatively positive relation of the trace elements in the weathered Ajali Sandstone samples with Fe_2O_3 and Al_2O_3 is an indication of the fact that the enrichment is related to secondary weathering/ferruginization process.

5. Discussion and inferences

According to Huntsman-Mapilaa et al. (2005), most commonly documented aspects of factors controlling chemical composition of siliciclastic sedimentary rocks are those of diagenesis, metamorphism, grain-size and density-controlled hydraulic sorting, mineralogical/petrological composition of the source rocks, degree of weathering of the source area and the tectonic setting.

5.1. Source area weathering

Furthermore, investigations of siliciclastic sedimentary rocks in several regions of the world show that their

chemical composition is largely dependent on the composition and the weathering conditions at the source rock area (Nesbitt and Young, 1989; Nesbitt et al., 1996). As demonstrated by Nesbitt and Young (1982), a measure of the degree of chemical weathering/alteration of the sediments' source rocks can be constrained by calculating the chemical index of alteration (CIA), where $CIA = \text{molar } [Al_2O_3 / (Al_2O_3 + CaO^* + Na_2O + K_2O)]$ while CaO^* represents the amount of CaO in silicate minerals only (i.e. excluding those of carbonates which are incidentally not presented in the fluvio-continental Ajali Sandstone as also indicated by very low content of CaO [0.1 – 0.04%]). Also, the proposed chemical index of weathering (CIW) of Harnois, 1988 is similar to the CIA with the exception of exclusion of K_2O in the equation ($CIW = \text{molar } [Al_2O_3 / (Al_2O_3 + CaO^* + Na_2O)]$). Usually, the CIA or CIW are interpreted in similar way with values of about 50 for unweathered (fresh) upper crust material and about 100 for highly weathered residual soils, with complete removal of alkali and alkaline-earth elements (McLennan et al., 1983; McLennan, 1993; Mongelli et al., 1996).

For this study, the estimated CIA and CIW (Table 3) yielded similar values in the range of 94.0 to 99.6 for fresh Ajali Sandstone samples and 98.3 to 99.6 for the ferruginized Ajali Sandstone samples. The unexpectedly high values of CIA and CIW for the fresh samples clearly indicate the fact that the primary source material(s) must have been subjected to substantially high degree of weathering and reworking that resulted in the removal of the ferromagnesian minerals and feldspars. However, the values of greater than 98 for the ferruginized samples are unequivocally indicative of weathering-ferruginization processes. Also, the plots of Al_2O_3 against CIA (Fig. 9A) and LOI against CIW (Fig. 9B) clearly discriminate between the fresh and ferruginized samples. As shown in Fig. 9, low values of Al_2O_3 and LOI in the fresh samples are a further confirmation of the loss during the primary weathering and sedimentary processes of the source rock materials. Furthermore, the MMI, i.e. the ratio of quartz to quartz + feldspar + rock fragments (Bhatia and Crook,

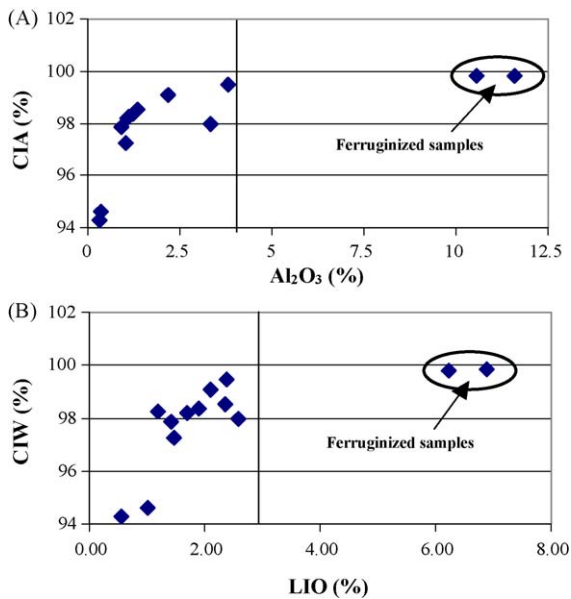


Fig. 9. Cross plots of weathering indices and other indicator parameters; A. Chemical Index of Alteration (CIA) against Al₂O₃. B. Chemical Index of Weathering (CIW) against LIO.

Fig. 9. Diagrammes représentatifs des indices d'altération et d'autres paramètres indicatifs. A. Index chimique d'altération (CIA) en fonction d' Al₂O₃. B. Index chimique d'altération (CIW) en fonction de LIO.

1986), for the fresh Ajali Sandstone samples (Table 2), ranges from 0.91 to 0.96 suggesting relatively high mineralogical maturity. MMI also correlates well with the estimated CIA and CIW values ($r=0.86$ and 0.82 , respectively), which is a reflection of the fact that the chemical compositions are, to a great extent, related to the petrographic modal data. Therefore, it can be concluded that the CIA and CIW values for the ferruginized samples reflect the recent (secondary) weathering–ferruginization process on one hand. On the other hand, those of the fresh samples are reflections of sediments derived from highly weathered and chemically matured terrain through primary weathering and reworking of the source materials.

From the results of the major element geochemistry of the Ajali Sandstone, the observed high proportion of quartz (> 90%), the relatively little but significant quantity of K-feldspar and the absence of the more chemically unstable plagioclase and other labile components (Table 3) suggest that the source rock was exposed to prolonged weathering and that the sediment is at least partly multicycle. Also, the observed mineralogical composition is concomitant with mainly granitic provenance while the occurrence of both common (unstrained) and metamorphic (strained) varieties could be attributed to source area that suggests a metamorphic and/or plutonic source for the sediments as also reported elsewhere by Basu et al. (1975); Dabbagh and Rogers (1983); Al-Harbi and Khan (2008). Again the composition of heavy minerals that are rich in ultrastable varieties such as zircon, rutile, and tourmaline is a pointer to a source from basement rock units, apparently from the Adamawa–Oban massif area to the east of the Anambra Basin. In addition, some of the observed sub-rounded

grains of the zircon and tourmaline may be attributable to prolonged abrasion and intrabasinal recycling from the adjacent Abakaliki Anticlinorium.

5.2. Provenance and tectonic settings

5.2.1. Evidence from major element geochemistry

The tectonic setting of the depositional environment is assumed to influence sedimentation, diagenesis and composition of sediments (Pettijohn et al., 1972; Bhatia, 1983; Chamley, 1990). A number of studies have used the detrital composition of sandstones to infer provenance and tectonic settings (Dickinson et al., 1983; Cavazza and Ingersoll, 2005; Greene et al., 2005). Hence, further clues for the provenance and tectonic settings can be inferred from the relative depletion in oxides like CaO, Na₂O (the most mobile phases) and enrichment of SiO₂, TiO₂, etc. (the most immobile elements). Using the typical quartz–feldspar–lithic fragment (Q–F–L) ternary diagram, adapted from Dickinson and Succec (1979) and presented in Fig. 10, the Ajali Sandstone can be clearly constrained to mature quartz arenite of continental cratonic block. This implies sandstones derived mainly from exposed shield/platform or from uplifted areas and deposited in stable sites (Taylor and McLennan, 1985; Potter, 1978, 1986). Therefore, with Q greater than 96% and negligible F and L components, the quartz arenite designation for the Ajali Sandstone is consistent with the passive margin (PM) setting or tectonically stable craton/shield source area mentioned earlier. This is consistent with the classification of Crook, 1974, which linked quartz-dominated sandstones (Q > 65%) to passive (Atlantic type) continental margin.

Furthermore, the discriminant function plot of Roser and Korsch (1988) as presented in Fig. 11a, defined four main provenance zones as: P1 = mafic igneous provenance;

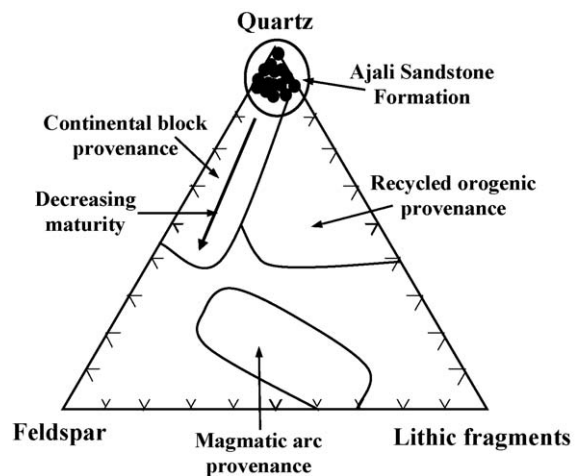


Fig. 10. Plot of Q–F–L ternary diagram of the Ajali Sandstone samples (adapted from Dickinson and Succec, 1979) indicating the Ajali Sandstone tectonic/provenance setting to be of mature continental block provenance.

Fig. 10. Diagramme ternaire Q–F–L des échantillons de grès d'Ajali (adapté d'après Dickinson et Succec, 1979) indiquant mise en place/tectonique du grès d'Ajali, comme celles d'un bloc continental mature.

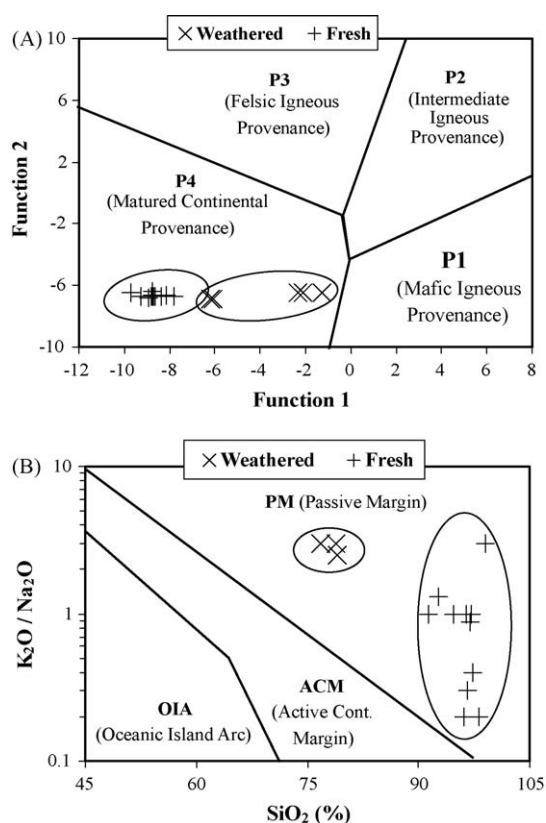


Fig. 11. A. Plots of Discriminant Functions 1 and 2 for the Maastrichtian Ajali Sandstone Formation (after Roser and Korsch, 1988). (P1 = mafic igneous provenance; P2 = intermediate igneous provenance; P3 = felsic igneous provenance; P4 = mature continental provenance). B. Plots of K_2O/Na_2O versus SiO_2 for the Maastrichtian Ajali Sandstone (after Roser and Korsch, 1986).

Fig. 11. A. Diagramme représentatif des fonctions discriminantes 1 et 2 pour la formation gréseuse maastrichtienne d'Ajali, selon Roser et Korsch, 1988. P1 = Source ignée mafique ; P2 = Source intermédiaire ignée ; P3 = Source ignée felsique ; P4 = Source continentale mature. B. Diagramme représentatif de valeurs de K_2O/Na_2O en fonction de SiO_2 pour le grès maastrichtien d'Ajali, après Roser et Korsch, 1986.

P2 = intermediate igneous provenance; P3 = felsic igneous provenance; and P4 = mature continental provenance. For this study, all of the Ajali Sandstone samples including the weathered samples lie within the zone of mature continental provenance setting (P4). Though the plot does not directly indicate a felsic igneous source, it can be concluded that the matured continental provenance is consistent with the PM setting and continental block provenance mentioned earlier. This assertion is further supported by the cross plot of K_2O/Na_2O versus SiO_2 (based on Roser and Korsch, 1986), as presented in Fig. 11b which indicates PM tectonic setting for the Ajali Sandstone. Consequently, it can be concluded that the adjacent Precambrian Basement units of the Oban–Adamawa massifs represent the provenance for the Ajali Sandstone. This is consistent with the assessment of Amajor (1987), and also supported by the westerly and southwesterly trending palaeo-current measurements presented by

Hoque and Ezepeue (1977). These also undoubtedly signify the easterly and northeasterly locations of the source areas. Furthermore, the apparently high values of CIA and CIW are clear indications of further contribution and significant geochemical control of the recycled materials from the uplifted extrusive/sedimentary units of the adjacent Abakaliki anticlinorium.

5.2.2. Evidence from trace element geochemistry

Over the years, the use of trace and major element geochemistry for discrimination of tectonic setting and provenance had been commonly applied to sedimentary units (e.g. Ronov et al., 1967; Roaldset, 1973; Ronov et al., 1974; Bhatia, 1983; Bhatia and Crook, 1986). Ohta (2004) reported that sedimentary processes do not only cause changes in the chemical composition of major components of a rock but also result in changes in the trace element budget. It has been reported that elements such as Ta, Th, Co, Ni, Y, Sc, Zr, Hf, Nb, Ti and REE are considered to have low mobility in transit (Taylor and McLennan, 1985; Bhatia and Crook, 1986; Andre et al., 1986; Shao et al., 2001) and hence useful in discriminating tectonic environments and source rock compositions (Bhatia, 1983; Roser and Korsch, 1986, 1988; Nesbitt et al., 1996). In addition, Co, Sc, Cr, Ni and Ti abundances are higher in mafic to intermediate rocks, whereas La, Th, Y and Zr are higher in felsic rocks (e.g., Taylor and McLennan, 1985; Cullers, 1995; Ishiga and Dozen, 1997; Shao et al., 2001). Hence, ratios such as La/Co, Th/Co, Zr/Cr, Th/Sc, La/Sc etc are considered to be good discriminators between mafic and felsic source rocks.

In this study, results of the ratios of some of the analyzed trace elements are presented in Table 5. It can be observed that Ti/Zr ratios range from 1.8 to 6.6 which is consistent with the values commonly recorded for felsic igneous rocks (< 20), unlike mafic igneous rocks that are characterized by higher values of greater than 50. Likewise, Zr/Cr range of 8.4 to 34.0 for the Ajali Sandstone is consistent with the value of greater than 2 for felsic igneous rocks compared to less than one for mafic type. Such high Zr/Cr ratio has been attributed to possible re-concentration of zircons by hydraulic sorting during the sedimentary processes. Furthermore, high values of La/Co (10 – 831), La/Sc (5 – 64), Th/Sc (4 – 53) and Zr/Cr (8 – 34) for the fresh Ajali Sandstone samples are clear indications of enrichment of La, Th, and Zr, thereby corroborating felsic source rock for the Ajali Sandstone. It can therefore be concluded that the relatively higher values of the above ratios suggest an evolutionary trend characterized by dominantly felsic source rock. The adjacent granitic basement rocks of the Adamawa/Oban massifs represent the felsic source rock lithology for the Ajali Sandstone. Nonetheless, the Y/Ni ratios of 0.38 – 5.1 (av. 1.8) for the Ajali Sandstone samples seem to overlap the range of values reported for both mafic and felsic igneous settings. The ratio Y/Ni is reported to be less than one in mafic igneous rocks compared to greater than 10 in felsic igneous rocks, except in some extensional granites/rhyolites (Huntsman-Mapilaa et al., 2005). The overlap of Y/Ni ratio between the felsic and mafic end-members suggests possible bimodal felsic-mafic rocks and/or intermediate rock sources. This can also be attributed to the interplay of

Table 5

Profiles of selected elemental ratios of the analyzed Ajali Sandstone.

Tableau 5

Profils de rapports entre éléments sélectionnés du grès d'Ajali analysé.

Sample Code ^a	Si/Al	Na/K	Al/(Ca+Na)	Fe/Mg	Zr/Hf	La/Sc	Th/Co	Y/Ni	La/Co	Ti/Zr	Th/Cr	Th/Sc	Zr/Cr
AJSt-01	299.8	0.3	16.5	7.0	74.1	39.8	262.0	0.4	398.0	5.2	0.5	26.2	8.4
AJSt-04a	86.7	1.0	56.0	29.0	65.2	5.0	8.6	2.1	10.0	5.5	0.5	4.3	25.6
AJSt-05a	88.7	3.3	54.5	21.0	64.4	6.2	10.6	1.0	17.0	4.6	0.6	3.9	34.0
AJSt-06a	280.4	5.0	17.5	17.0	76.4	63.9	390.0	0.2	831.0	1.8	0.3	30.0	23.7
AJSt-09a	43.5	1.0	109.0	59.0	58.1	11.4	31.7	5.1	54.1	5.8	0.4	6.7	20.9
AJSt-10a	72.3	5.0	66.5	3.0	79.7	30.3	688.0	3.5	394.0	3.5	1.4	52.9	23.8
AJSt-12	105.7	2.5	46.0	17.0	58.0	6.1	68.1	0.2	64.0	6.6	0.7	6.5	22.6
AJSt-05c (W)	7.5	0.3	527.0	81.3	73.9	4.3	6.4	2.0	17.8	7.6	0.2	1.5	15.5
AJSt-11a (W)	24.1	1.0	189.5	97.0	65.8	8.2	12.0	1.1	22.6	5.6	0.5	4.4	25.2
AJSt-14a (W)	6.6	0.3	578.5	89.3	60.7	3.9	5.3	1.4	11.5	7.8	0.3	1.8	13.6
Mean (overall)	101.5	2.0	166.1	42.1	67.6	17.9	148.3	1.7	182.0	5.4	0.5	13.8	21.3
Mean (fresh)	139.6	2.6	52.3	21.9	68.0	23.2	208.4	1.8	252.6	4.7	0.6	18.6	22.7

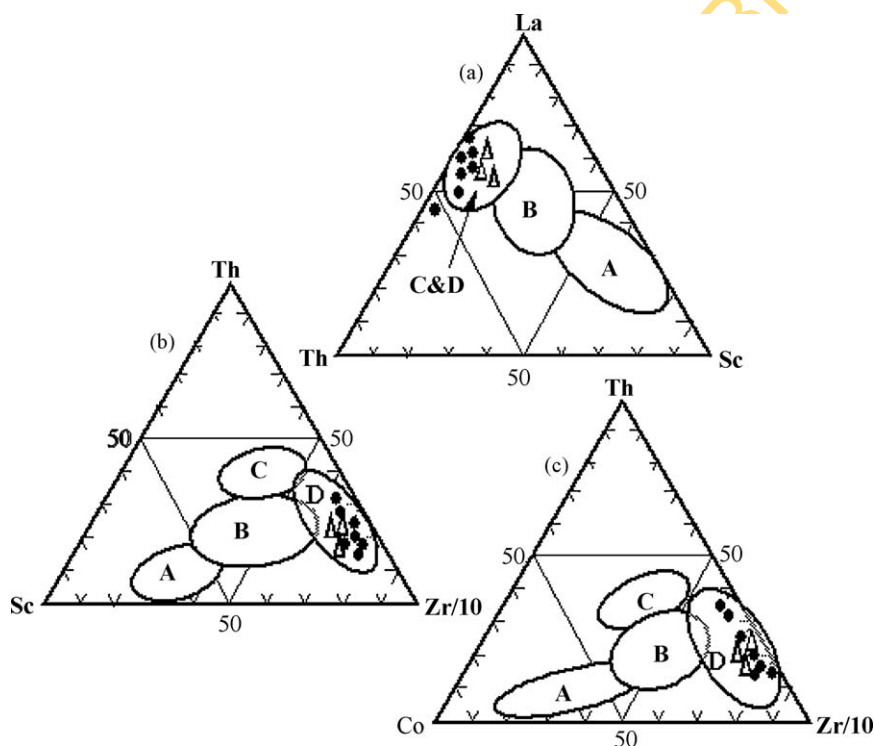
^a Sample names as in Table 3 while weathered/ferruginized samples marked with (W).**Fig. 12.** Plot of the Ajali Sandstone samples in the tectonic discrimination diagrams; (a) La–Sc–Th, (b) Th–Sc–Zr/10 and (c) Th–Co–Zr/10 (after Bhatia and Crook, 1986): A. Oceanic island arc. B. Continental island arc. C. Active continental margins. D. Passive continental margins.

Fig. 12. Croquis représentatif des échantillons de grès d'Ajali dans les diagrammes de discrimination tectonique. (a) La–Sc–Th ; (b) Th–Sc–Zr/10 ; (c) th–Co–Zr/10 selon Bhatia et Crook, 1986 : A. Arc insulaire océanique. B. Arc insulaire continental. C. Marges continentales actives. D. Marges continentales passives.

contributions from Adamawa/Oban Massif area and the extrusive units of the uplifted Abakaliki area.

Using discriminant plots of Bhatia and Crook (1986), samples from the study area plot in both active continental margin (ACM) and PM settings (Fig. 12a). However, both Th–Sc–Zr/10 and Th–Co–Zr/10 ternary plots (Fig. 12b and c) revealed exclusively PM setting of the source area of the Ajali Sandstone. These plots support at least a siliciclastic source for Ajali Sandstone and are also indicative of tectonically stable felsic (granitic)

craton/shield source area, which is known to be characterized by quartz arenites (Pettijohn, 1975). This is consistent with the relatively low concentrations of the transitional elements (such as Cr, Co, Ni, and V) reflecting negligible input of mafic provenance, as also reported by Osaie et al., 2006; Akarish and El-Gohary, 2008. It can therefore be deduced from the trace element geochemistry that the source area of the Ajali Sandstone is related to predominantly felsic rocks characterized by stable continental environment with possible contribution of

recycled materials from intrusive units of the uplifted Abakaliki Anticlinorium as pointed out earlier.

There is no doubt that several factors control the chemical composition of elements in siliciclastic sedimentary rocks like the Ajali Sandstone. Summarizing the foregoing discussions, it can be concluded that the unconsolidated friable nature of the Ajali Sandstone clearly excludes metamorphic remobilization as a controlling process. However, possible interplay of grain-size and density-controlled hydraulic sorting on one hand and the obvious geochemical/mineralogical composition and degree of weathering of the source area on the other hand can be regarded as dominant controlling factors for the Ajali Sandstone.

6. Summary and conclusion

In this study, assessments of the textural and geochemical characteristics of Ajali Sandstone were undertaken. The results indicate the Ajali Sandstone is characterized by predominantly medium–fine sand fractions, which are typically whitish in colour and cross-stratified in places. Statistical parameters show that the sediments are products of fluvial/river channel system. Furthermore, the estimated weathering indices revealed that the CIA and CIW values for the ferruginized samples (98.3 – 99.6) reflect the recent (secondary) weathering-ferruginization process, while that of the fresh samples (86.8 – 99.6) are reflections of the primary weathering and recycling of the source materials of the Ajali Sandstone during transportation and sedimentary process.

Arising from elemental compositions, binary plots (e.g., Cr–Ni, V–Ni, Ni–SiO₂, Cr–SiO₂, K₂O–Al₂O₃ and Na₂O–Al₂O₃), inter-elements ratios such as Zr/Cr, Y/Ni, Th/Sc, La/Sc and La/Co as well as the corresponding source-rock discrimination diagrams (e.g., Th–Sc–Zr and La–Th–Sc Th–Co–Zr), it can be deduced that the sediments were sourced from a felsic igneous-dominated continental setting. Consequently, the provenance is constrained to the adjacent Precambrian Basement units of Adamawa–Oban massif upland and adjacent Abakaliki anticlinorium. Again, the friable nature of the sediments is in conformity with fluviocontinental setting and clearly excludes any possible metamorphic remobilization process. However, the overall assessments presented in this study, suggest interplay of geochemical-mineralogical compositions and the degree of weathering of the source rock area. This is consistent with the statistical factor analysis of the geochemical data and other associated variables, which revealed geochemical controls on the weathering and provenance/tectonic setting of the source areas of the Ajali Sandstone.

Acknowledgements

The assistance and help of Mr. K. Watanabe in the course of laboratory analytical measurements is greatly appreciated. The sponsorship of the JSPS for the first author during the research study visit to Japan as well as the moral support of Prof. S. Onodera are also acknowledged. This manuscript benefited from the useful comments and

suggestions of two anonymous reviewers, for which the authors hereby greatly appreciated with thanks.

References

- Adediran, S.A., Adegoke, O.S., Oshin, I.O., 1991. The continental sediments of the Nigerian Coastal Basins. *J. Afr. Earth Sci.* 12 (1–2), 79–84.
- Akarish, A.I.M., El-Gohary, A.M., 2008. Petrography and geochemistry of Lower Paleozoic sandstones, East Sinai, Egypt: Implications for provenance and tectonic setting. *J. Afr. Earth Sci.* 52, 43–54.
- Al-Harbi, O.A., Khan, M.M., 2008. Provenance, diagenesis, tectonic setting and geochemistry of Tawil Sandstone (Lower Devonian) in Central Saudi Arabia. *J. Asian Earth Sci.* 33, 278–287.
- Amajor, L.C., 1987. Paleocurrent, petrography and provenance analyses of the Ajali Sandstone (Upper Cretaceous), southeastern Benue Trough, Nigeria. *Sedim. Geol.* 54, 47–60.
- Andre, L., Deutsch, S., Hertogen, J., 1986. Trace element and Nd isotopes in shales as indexes of provenance and crustal growth: the early paleozoic from the Brabant massif. *Belgium Chem. Geol.* 57, 101–115.
- Basu, A., Young, S., Suttner, L.J., James, W.C., Mack, C.H., 1975. Reevaluation of the use of undulatory extinction and polycrystallinity in detrital quartz for provenance interpretation. *J. Sedim. Petrol.* 45, 873–882.
- Benkheilil, J., 1986. Structure and Geodynamics Evolution of the intracontinental Benue-Trough (Nigeria), Thesis, University of Nice 202p. Pub. Elf (Nig.) Ltd.
- Bhatia, M.R., 1983. Plate tectonics and geochemical composition of sandstones. *J. Geol.* 91, 611–627.
- Bhatia, M.R., Crook, K.A.W., 1986. Trace element characteristics of graywackes and tectonic setting discrimination of sedimentary basins. *Contrib. Mineral. Petrol.* 92, 181–193.
- Cavazza, W., Ingersoll, R., 2005. Detrital modes of the Ionian forearc basin fill (Oligocene–Quaternary) reflect the tectonic evolution of the Calabria–Peloritani terrane (southern Italy). *J. Sed. Res.* 75, 268–279.
- Chamley, H., 1990. *Sedimentology*. Springer-Verlag, Berlin.
- Crook, K.A.W., 1974. Lithostratigraphy and geotectonic: The significance of composition variation in flysch arenites (graywackes). In: Dott, R.H., Shaver, R.H. (Eds.), *Modern and Ancient Geosynclinal Sedimentation*, 19; Soc. Econ. Paleontol. Mineral. Spec. Pub. pp. 304–310.
- Cullers, R.L., 1995. The controls of the major- and trace-element evolution of shales, siltstones and sandstones of Ordovician to Tertiary age in the Wet Mountains region Colorado USA. *Chem. Geol.* 123, 107–131.
- Cullers, R.L., 2000. The geochemistry of shales, siltstones and sandstones of Pennsylvanian–Permian age, Colorado, USA: Implications for provenance and metamorphic studies. *Lithos* 51, 181–203.
- Dabbagh, M.E., Rogers, J.J., 1983. Depositional environments and tectonic significance of the Wajid Sandstone of southern Saudi Arabia. *J. Afr. Earth Sci.* 47–57.
- Das, B.K., Haake, B., 2003. Geochemistry of Rewalsar Lake sediments, Lesser Himalaya, India: Implications for source-area weathering, provenance and tectonic setting. *J. Geosci.* 7, 299–312.
- Dickinson, W.R., 1970. Interpreting detrital modes of Greywacke and Arkose. *J. Sedim. Petrol.* 40, 695–707.
- Dickinson, W.R., Suczek, C.A., 1979. Plate tectonics and sandstone compositions. *Am. Assoc. Petr. Geol. Bull.* 63, 2171.
- Dickinson, W.R., Beard, L.S., Brakenridge, G.R., Erjavec, J.L., Ferguson, R.C., Inman, K.F., et al., 1983. Provenance of North-American Phanerozoic sandstones in relation to tectonic setting. *Bull. Am. Geol. Soc.* 94, 222–235.
- Folk, R.L., Ward, W.C., 1957. Brazo river bar: A study of the significance of grain size parameters. *J. Sedim. Geol.* 27, 3–26.
- Folk, R.L., 1974. *Petrology of Sedimentary Rocks*. Hemphill Publication Co, Austin, Texas, USA.
- Friedman, G.M., 1967. Dynamic process and statistical parameters compared for size frequency distribution of beach and river sands. *J. Sedim. Petrol.* 37, 327–354.
- Friedman, G.M., 1969. Differences in size distribution of populations of particles among sands of various origins. *Sedimentology* 26, 3–32.
- Gazzi, P., 1966. Le arenarie del flysch sopracretaceo dell'Appennino modenese, correlazioni con il flysch di Monghidoro. *Miner. Petrogr. Acta* 12, 69–97.
- Getaneh, W., 2002. Geochemistry provenance and depositional tectonic setting of the Adigrat Sandstone northern Ethiopia. *J. Afr. Earth Sci.* 35, 185–198.
- Goetze, J., 1998. Geochemistry and provenance of the Altendorf feldspathic sandstone in the Middle Bunter of the Thuringian basin (Germany). *Chem. Geol.* 150, 43–61.

- Greene, T.J., Carroll, A.R., Wartes, M., Graham, S.A., Wooden, J.L., 2005. Integrated provenance analysis of a complex orogenic terrane: Mesozoic uplift of the Bogda Shan and Inception of the Turpan-Hami Basin, NW China. *J. Sedim. Res.* 75, 251–267.
- Harnois, L., 1988. The CIW index: a new Chemical Index of Weathering. *Sedim. Geol.* 55, 319–322.
- Hoque, M., Ezepe, M.C., 1977. Petrology and Palaeogeography of the Ajali Sandstone. *J. Mining Geol.* 14 (1), 6–22.
- Huntsman-Mapilaa, P., Kampunzuc, A.B., Vinkc, B., Ringrosea, S., 2005. Cryptic indicators of provenance from the geochemistry of the Okavango Delta sediments, Botswana. *Sedim. Geol.* 174, 123–148.
- Ingersoll, R.V., Bullard, T.F., Ford, R.L., Grimm, J.P., Pickle, J.D., Sares, S.W., 1984. The effects of grain size on data modes: a test of the Gazzi-Dickinson point-counting method. *J. Sedim. Petrol.* 46, 620–632.
- Ishiga, H., Dozen, K., 1997. Geochemical indications of provenance change as recorded in Miocene shales: opening of the Japan Sea, San'in region, Southwest Japan. *Mar. Geol.* 144, 211–228.
- Jin, Z., Li, F., Cao, J., Wang, S., Yu, J., 2006. Geochemistry of Daihai Lake sediments, Inner Mongolia, north China: Implications for provenance, sedimentary sorting and catchment weathering. *Geomorphology* 80, 147–163.
- Ladipo, K.O., 1986. Tidal shelf depositional model for the Ajali Sandstone, Anambra Basin, southern Nigeria. *J. Afr. Earth Sci.* 5 (2), 177–185.
- Ladipo, K.O., 1988. Paleogeography, sedimentation and tectonics of the Upper Cretaceous Anambra basin, southeastern Nigeria. *J. Afr. Earth Sci.* 7 (5–6), 865–871.
- McLennan, S.M., 1993. Weathering and global denudation. *J. Geol.* 101, 295–303.
- McLennan, S.M., Taylor, S.R., Eriksson, K.A., 1983. Geochemistry of Archean shales from the Pilbara Supergroup, Western Australia. *Geochim. Cosmochim. Acta* 47, 1211–1222.
- Mongelli, G., Cullers, R.L., Muelheisen, S., 1996. Geochemistry of Late Cretaceous-Oligocene shales from the Varicolori Formation, southern Apennines, Italy: implications for mineralogical, grain-size control and provenance. *Eur. J. Mineral.* 8, 733–754.
- Murat, R.C., 1972. Stratigraphy and Palaeogeography of the Cretaceous and Lower Tertiary in southern Nigeria. In: Dessauvage, T.F.J., Whiteman, A.J. (Eds.), *African geology* 251–266.
- Nesbitt, H.W., Young, G.M., 1982. Early Proterozoic climates and plate motions inferred from major element chemistry of lutites. *Nature* 299, 715–717.
- Nesbitt, H.W., Young, G.M., 1989. Formation and diagenesis of weathering profiles. *J. Geol.* 97, 129–147.
- Nesbitt, H.W., Young, G.M., McLennan, S.M., Keays, R.R., 1996. Effect of chemical weathering and sorting on the petrogenesis of siliciclastic sediments, with implications for provenance studies. *J. Geol.* 104, 525–542.
- Ohta, T., 2004. Geochemistry of Jurassic to Earliest Cretaceous deposits in the Nagato Basin, SW Japan: implication of factor analysis to sorting effects and provenance signatures. *Sedim. Geol.* 171, 159–180.
- Okagbue, C.O. 1988. Hydrology and chemical characteristics of surface and Groundwater Resources of the Okigwe Area and Environs, Imo State, Nigeria. In: C.O. Ofoegbu (Ed.), *Groundwater and Mineral Resources of Nigeria*; Friedr. Vieweg & Sohn, Braunschweig/Wiesbaden. pp. 3 – 15.
- Olugbemi, R.O., Nwajide, C.S., 1997. Grain-size distribution and particle morphogenesis as signatures of depositional environments of Cretaceous (non-ferruginous) facies in the Bida Basin, Nigeria. *J. Mining Geol.* 33 (2), 89–101.
- Osae, S., Asiedu, D.K., Banoeng-Yakubu, Koeberl, C., Dampare, S.B., 2006. Provenance and tectonic setting of Late Proterozoic Buem sandstones of southeastern Ghana; Evidence from geochemistry and detrital modes. *J. Afr. Earth Sci.* 44, 85–96.
- Pettijohn, F.J., 1963. Chemical composition of sandstones excluding carbonate and volcanic sands. In: *Data of geochemistry*, 6th Ed; US Geological Survey Professional Paper, 44a-S, 19 p.
- Pettijohn, F.J., 1975. *Sedimentary Rocks*. Harper and Row, New York, 628 p.
- Pettijohn, F.J., Potter, P.E., Siever, R., 1972. *Sand and Sandstones*. Springer-Verlag, New York, USA.
- Potter, P.E., 1978. Petrology and chemistry of modern Big River sands. *J. Geol.* 86, 423–449.
- Potter, P.E., 1986. South America and a few grains of sand: Part 1 – beach sands. *Jour. Geol.* 94, 301–319.
- Reyment, R.A., 1965. *Aspects of Geology of Nigeria*. University of Ibadan, Press, 145 p.
- Roaldset, E., 1973. Rare earth elements in Quaternary clays of the Numedal area, southern Norway. *Lithos* 6, 349–357.
- Ronov, A.B., Balashov, Y.A., Migdisov, A.A., 1967. Geochemistry of rare earths in the sedimentary cycle. *Geochem. Int.* 4, 157–172.
- Ronov, A.B., Balashov, Y.A., Girin, Y.P., Bratishko, R.K.H., Kazakov, G.A., 1974. Regularities of rare earth element distribution in the sedimentary shell and in the crust of the earth. *Sedimentology* 21, 171–193.
- Roser, B.P., Korsch, R.J., 1986. Determination of tectonic setting of sandstone-mudstone Suites using SiO₂ content and K₂O/Na₂O ratio. *J. Geol.* 635–650.
- Roser, B.P., Korsch, R.J., 1988. Provenance signatures of sandstone-mudstone suites determined using discriminant function analysis of major-element data. *Chem. Geol.* 67, 119–139.
- Shao, L., Stettenger, K., Garbe-Schoenberg, C.D., 2001. Sandstone petrology and geochemistry of the Turpan basin (NW China): implications for the tectonic evolution of a continental basin. *J. Sedim. Res.* 71, 37–49.
- Simpson, A., 1955. The Nigerian coalfield: The geology of parts of Owerri and Benue Provinces. *Bull. Geol. Surv. Niger.* 24, 85 p.
- Tattam, C.M., 1944. A Review of Nigerian Stratigraphy. *Rep. Geol. Surv. Niger.* 27–46.
- Taylor, S.R., McLennan, S.M., 1985. *The Continental Crust: Its Composition and Evolution*. Blackwell Scientific, Oxford (312 p).
- Tijani, M.N., Okunlola, O.A., Abimbola, A.F., 2006. Lithogenic concentrations of trace metals in soils and saprolites over crystalline basement rocks: A case study from SW Nigeria. *J. Afr. Earth Sci.* 46, 427–438.
- Tijani, M.N., Nton, M.E., 2009. Hydraulic, textural and geochemical characteristics of the Ajali Formation, Anambra Basin, Nigeria: implication for groundwater quality. *Environ. Geol.* 56, 935–951.
- Uma, K.O., Onuoha, K.M., 1988. Groundwater fluxes and gully Development in S.E. Nigeria. In: Ofoegbu, C.O. (Ed.), *Groundwater and Mineral Resources of Nigeria*. Friedr. Vieweg & Sohn, Braunschweig/Wiesbaden, pp. 39–59.
- Wronkiewicz, D.J., Condie, K.C., 1987. Geochemistry of Archean shales from the Witwatersrand Supergroup, South Africa: source-area weathering and provenance. *Geochim. Cosmochim. Acta* 51, 2401–2416.
- Wronkiewicz, D.J., Condie, K.C., 1990. Geochemistry and mineralogy of sediments from the Ventersdorp and Transvaal Supergroups, South Africa: Cratonic evolution during the Early Proterozoic. *Geochim. Cosmochim. Acta* 54, 343–354.